

# General Oscillator Characterization Using Linear Open-Loop $S$ -Parameters

Mitch Randall and Terry Hock, *Member, IEEE*

**Abstract**—From a practical standpoint, oscillator design using linear open-loop  $S$ -parameters is attractive to designers due to the ease of use and widespread availability of linear  $S$ -parameter-based analysis software. However, the easiest and, therefore, most common approach is based on intuition and rules of thumb. The intent of this paper is to obtain quantitative expressions that characterize oscillator performance in terms of the linear open-loop  $S$ -parameters. A characteristic equation is derived that determines oscillator stability. The Nyquist stability criteria can be applied to this equation directly from the open-loop Bode plot. A closed-loop gain parameter is derived, which describes how the open-loop circuit self-connects. From this parameter, the startup time, oscillation frequency, and loaded  $Q$  can be predicted. A prediction of actual oscillation frequency can be made based on a simple oscillator model with known saturation characteristics. It will be shown under what conditions these expressions simplify to more readily applicable forms. In many cases, the designer can adjust analysis parameters to allow the use of the simplified expressions.

**Index Terms**—Analysis, closed-loop gain, linear design, oscillator, oscillator stability,  $S$ -parameters.

## I. INTRODUCTION

ONE METHOD of designing and analyzing an oscillator is to consider it as a closed-loop circuit composed of an amplifier and a tuned network. A technique called “transmission analysis using virtual ground” [1] allows this method to be readily applied to almost any oscillator in a straightforward way. This approach is advantageous over techniques such as negative resistance [2]–[4], closed-loop analysis [5], open-loop Bode plots [6], nonlinear  $S$ -parameters [7], and numerous other variations that can be difficult to apply, or difficult to interpret, or both.

The virtual-ground technique calls for redefining a virtual ground in an oscillator circuit such that the amplifier and tuned network can be identified. Once the feedback mechanism is identified, the loop is opened to create a two-port network. Closed-loop oscillator performance, i.e., frequency, gain margin, and loaded  $Q$ , is inferred from the magnitude, phase, and group delay of the forward scattering parameter  $S_{21}$  of the open-loop network. The virtual-ground approach can uncover the underlying operational principle of an oscillator that may not be obvious in the original circuit; the intuition gained could inspire a new generation of optimized designs. In addition, no specialized software tools are required to apply this technique.

Manuscript received July 14, 1999; revised September 18, 2000. This work was supported by the National Science Foundation.

The authors are with The National Center for Atmospheric Research Boulder, CO 80303 USA (e-mail: mitch@ucar.edu; hock@ucar.edu).

Publisher Item Identifier S 0018-9480(01)03991-6.

It can be applied using only standard network analysis software, which is ubiquitous in the RF engineering community.

However, the use of  $S_{21}$  directly for characterization is not exact. For example, the frequency at which the phase of  $S_{21}$  crosses zero is not generally the frequency of oscillation. These differences are due to the difference between the terminating impedances used for analysis, and the impedances presented when the loop is closed.

The purpose of this paper is to provide expressions and techniques that can be used to better interpret the results of open-loop  $S$ -parameter analysis for oscillator design. The full form of the expressions offers insight into the origin of many of the rules of thumb commonly used in practice. These common techniques are used because of their convenience and intuitive nature. With their formal derivation revealed, these rules can be applied with greater accuracy. These tools augment the virtual-ground method, resulting in an accurate and widely applicable oscillator design technique.

We start by formally analyzing the closed-loop response of a general network to obtain a characteristic equation. The Nyquist test can be applied to the Bode plot of the characteristic equation. This closely resembles the practice of designing for greater than unity gain at the phase zero crossing. However, the formality includes additional rules that reveal the limitations of the more common practice.

A simple feedback oscillator model is described that is assumed to model a general oscillator. The characteristics of the model are readily computed and serve as a reference. We then introduce a parameter  $G$ , which represents the gain of a general network when it is self-terminated. It is found that  $G$  is governed by the same characteristic equation derived earlier. We see that applying  $G$  to the model oscillator accurately reveals its behavior. The full technique for analyzing an open-loop network is then detailed. We then discuss practical approximations that can be used and the various conditions under which they are valid. The technique is applied to a practical oscillator and the results are compared to a SPICE simulation.

## II. OSCILLATOR STABILITY

It has been shown that excess gain at the phase zero crossing is necessary, but not sufficient to guarantee oscillations [8], [9]. However, the Nyquist criteria from classical control theory can be used to uniquely determine stability. Nguyen and Meyer [9] provide an excellent description of the issues involved as they relate to high-frequency oscillators. Here, we extend this technique for use with linear two-port  $S$ -parameter analysis.

Any oscillator can be decomposed into a two-port network connected closed loop. We can investigate the startup stability

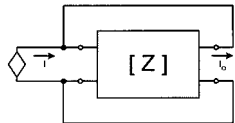


Fig. 1. Oscillator network with source. The characteristic equation and, therefore, stability of the network, is determined by considering the transfer function of the oscillator with an artificial current source.

by analyzing the response of the network when connected as shown in Fig. 1. Using *Z*-parameters, it can be easily shown that the transfer characteristic is given by

$$\frac{I_o}{I} = \frac{z_f - z_i}{z_i - z_r - z_f + z_o}.$$

This can be rewritten in terms of *S*-parameters as [10]

$$\frac{I_o}{I} = \frac{S_{22} - S_{11} + 2S_{21} - S_{12}S_{21} + S_{11}S_{22} - 1}{1 - (S_{12} + S_{21} - S_{12}S_{21} + S_{11}S_{22})}.$$

We are not so much interested in the transfer function as in the resulting characteristic equation since, in practice, the driving current source is set to zero. The characteristic equation is

$$1 - (S_{12} + S_{21} - S_{12}S_{21} + S_{11}S_{22}) = 0.$$

It is interesting to note that since the characteristic equation derived makes no assumptions about the nature of the oscillations, it is also applicable to negative resistance oscillator analysis. In that case,  $S_{12}$  and  $S_{21}$  are zero and the equation reduces to the familiar form  $S_{12}S_{21} = 1$ .

We can now apply the Nyquist criteria to the characteristic equation to determine stability and guarantee oscillator startup. As a reminder, the Nyquist criteria for oscillation states that the polar open-loop response and its image must make at least one net clockwise encirclement of the point  $1 + i0$  as frequency is increased. A more concise description with examples can be found in any of a number of control theory textbooks such as [11].

The Nyquist diagram, which is just the open-loop response plotted in polar coordinates, is the most convenient format to check for encirclement. The Bode plot contains this same information, but in Cartesian coordinates. Therefore, in principle, the Nyquist criteria can be applied equally well to the Bode plot. This form is less convenient in the most general case. However, in almost all practical oscillators, it is easy to use a the Bode plot to check the Nyquist criteria at a glance.

On the Bode plot, “encirclement” is as follows. When the log magnitude gain is positive at the phase crossing, negative phase slope corresponds to clockwise rotation; positive phase slope corresponds to counterclockwise rotation. When the gain is negative, those directions are reversed. For oscillation, clockwise phase zero crossings must outnumber counterclockwise phase zero crossings. For the vast majority of oscillators, there is only one phase zero crossing and it has negative slope (see Fig. 2). In this case, the formal Nyquist test simplifies to the common practice of designing for positive gain at the phase zero crossing.

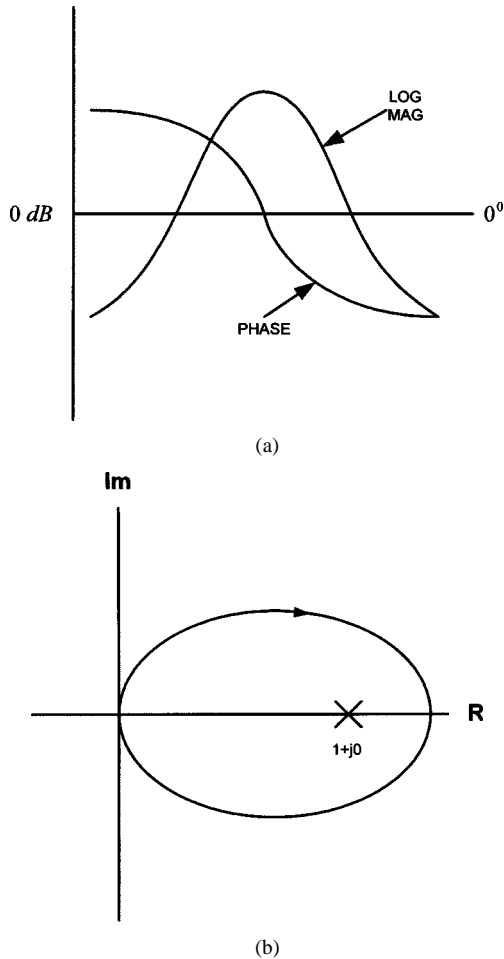


Fig. 2. Comparison of Bode plot and Nyquist diagram. (a) A typical oscillator has a single phase zero crossing with negative slope and positive gain. (b) The same response is shown in polar coordinates (a Nyquist diagram).

### III. OSCILLATOR STARTUP

A simple interpretation of the open-loop characteristics allows the startup time to be estimated. In addition, this interpretation helps to explain the underlying reason why the sign of the phase slope plays a critical role in stability.

Consider an open-loop network of an oscillator at the frequency of the phase zero crossing  $\omega_\phi$  with gain  $G_0$  and a given time delay  $\tau$ . To close the loop is to impose the boundary condition that the output be equal to the input. Assuming the solution is an exponentially increasing sine wave, and equating input and output, we have

$$e^{\alpha t} \sin(\omega_\phi t) = G_0 e^{\alpha(t-\tau)} \sin(\omega_\phi(t-\tau) + \theta).$$

We focus on the oscillation frequency, which occurs at the phase zero crossing. The phase zero crossing implies that  $\theta$  is such that the following condition is satisfied:

$$\sin(\omega_\phi t) = \sin(\omega_\phi(t-\tau) + \theta).$$

Therefore, the exponentially growing sine function solves the boundary conditions provided

$$\alpha = \frac{1}{\tau} \ln G_0.$$

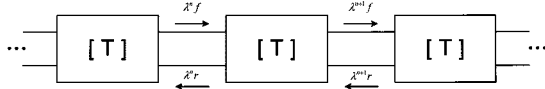


Fig. 3. Infinite chain of identical networks. The ratio of the forward ( $f$ ) and reverse ( $r$ ) waves is identical at each junction, but the amplitude of the waves increases by a factor of  $\lambda$  with each network.

In other words, after a delay  $\tau$  and a gain  $G_0$ , the input will equal the output. In this context, the time delay can be approximated by the group delay  $\tau_g$ , which is defined as the phase slope [12]. The 10–90 rise time can, therefore, be estimated as

$$t_r \approx \frac{\ln 9}{\ln G_0} \tau_g = \frac{19.1}{G_{0\text{dB}}} \tau_g = -\frac{19.1}{G_{0\text{dB}}} \frac{\partial \varphi}{\partial \omega}$$

where  $G_{\text{dB}}$  is the open-loop gain expressed in decibels. The relationship between the group delay and the phase slope sheds light on its importance in the Nyquist criterion. A negative phase slope corresponds to a time delay. If the gain is positive and there is a time delay, an exponentially increasing sine wave solves the boundary conditions. On the other hand, a positive phase slope corresponds to a time advance. If the gain is positive and there is a time advance, an exponentially *decreasing* sine wave solves the boundary conditions, implying stability at that frequency.

#### IV. CHARACTERIZING OSCILLATOR OPEN-LOOP BEHAVIOR

To correctly characterize a closed-loop network using the open-loop behavior, the effects of the impedance mismatch at the connection point must be included. To do this, we consider the behavior of an infinite number of identical open-loop networks connected end to end, as shown in Fig. 3. The reflection coefficients will be identical at each junction. However, the signal at one junction will differ from the signal at an adjacent junction by some gain and phase. Using transfer scattering parameters, this set of conditions can be stated as

$$\begin{bmatrix} T_{11} & T_{12} \\ T_{21} & T_{22} \end{bmatrix} \begin{bmatrix} r \\ f \end{bmatrix} = \lambda \begin{bmatrix} r \\ f \end{bmatrix}$$

where  $f$  and  $r$  are the forward and reflected wave variables, respectively, at each junction, and  $\lambda$  is the ratio of the signal at one junction to the signal at an adjacent junction. This is recognized as an eigenvalue equation.  $\lambda$  can take on two eigenvalues given by

$$\lambda = \frac{1}{G} = \frac{(T_{11}+T_{22}) \pm \sqrt{(T_{11}+T_{22})^2 - 4(T_{11}T_{22} - T_{12}T_{21})}}{2}.$$

The two eigenvalues represent possible right- and left-moving waves. Feedback oscillators are predominantly built around a unilateral device so one mode corresponds to an exponentially increasing signal and the other corresponds to an exponentially decaying signal. We, therefore, discard the minus sign from further analysis. The eigenvalue  $\lambda$  can be interpreted as the reciprocal of the forward open-loop gain  $G$ . In terms of  $Z$ -parameters

$$G = \frac{2g}{1 + \sqrt{1 - 4(z_r/z_f)g^2}}$$

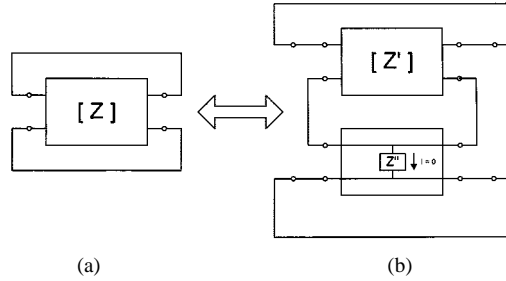


Fig. 4. Equivalent networks. (a) Any network can be decomposed into the sum of (b) two series networks. In the steady state, no current will flow through  $Z''$  and, therefore, it can be neglected.

where

$$g = \frac{z_f}{z_i + z_o}.$$

From this form, it is seen that  $G$  has the virtue of being independent of the test-set normalizing impedance.

A simplification occurs if the reverse impedance parameter  $z_r$  of the network is zero. A general open-loop oscillator network can always be transformed in such a way to allow this simplification by the following argument. A general network can be represented by the series combination of two networks, as shown in Fig. 4, such that

$$Z = Z' + Z''$$

where  $Z$  is the impedance matrix of the general network, and  $Z'$  and  $Z''$  are the impedance matrices of the transformed network and the lumped impedance element, respectively. It is evident that when the combined network is connected as an oscillator as shown (i.e., the input is connected to the output), no current will flow through the lumped impedance element. Operation of the oscillator is, therefore, independent of the lumped impedance element  $Z''$ . The value of the lumped impedance element can be chosen such that the transformed network  $Z'$  has a reverse transfer impedance of zero. The transformed network is then given by

$$Z' = \begin{bmatrix} z_i - z_r & 0 \\ z_f - z_r & z_o - z_r \end{bmatrix}.$$

Based on the network  $Z'$ ,  $G$  is then given by

$$G = g = \frac{z_f - z_r}{z_i + z_o - 2z_r}.$$

Expressed in terms of  $S$ -parameters

$$G = \frac{S_{21} - S_{12}}{1 - S_{11}S_{22} + S_{12}S_{21} - 2S_{12}}.$$

A special condition of interest arises when the open-loop gain  $G$  takes on a value of one at some point in the complex plane. This operating point satisfies the boundary conditions imposed by a closed loop. Specifically, at this point, the input is equal to the output. From classical control theory, this point corresponds to a pole in the closed-loop transfer function. The condition that  $G = 1$  is satisfied whenever

$$1 - (S_{12} + S_{21} - S_{12}S_{21} + S_{11}S_{22}) = 0$$

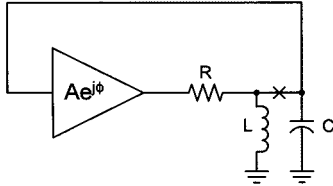


Fig. 5. Model oscillator. It is assumed that an oscillator can be modeled as an amplifier and a single tuned network. The split point used in the analysis is shown.

which is just the characteristic equation from the earlier *Z*-parameter analysis. In other words, the open-loop gain  $G$  describes the poles of a single closed-loop network in agreement with the earlier *Z*-parameter analysis. It is, therefore, possible and convenient to determine stability by applying the Nyquist criteria directly to the parameter  $G$ .

## V. FEEDBACK OSCILLATOR MODEL

In order to predict oscillator performance and compare results against a standard, we introduce a simple oscillator model, as shown in Fig. 5. We postulate that at the frequency of oscillation, a typical resonator is well approximated by an *LC* tank. At this frequency, the nonresonant part of the network is lumped into the gain and phase of an amplifier  $Ae^{i\phi}$ , where  $A$  and  $\phi$  are real numbers. The network is assumed to have negligible gain in the reverse direction. This model will serve as a reference by which to validate the accuracy of parameters computed with the parameter  $G$ .

Using the *Z*-parameter derivation above, the closed-loop transfer function of the network is given by

$$\frac{I_o}{I} = -\frac{\omega_n^2 + i\omega(\omega_n/Q_n)(1 - Ae^{i\phi})}{\omega_n^2 - \omega^2 + i\omega(\omega_n/Q_n)(1 - Ae^{i\phi})}$$

where  $Q_n = \omega_n RC$  and  $\omega_n^2 = 1/LC$

A practical oscillator must have an open-loop gain greater than unity to guarantee reliable starting. In the steady state, the oscillator saturates so that the gain is exactly unity. In this model, saturation is assumed to affect the gain  $A$ , but not the phase  $\phi$ , which is assumed to remain fixed. Given this, in steady state,  $A$  then saturates to a value of  $\sec(\phi)$  at a frequency

$$\omega_o = \omega_n \left( \frac{\tan(\phi)}{2Q_n} + \sqrt{1 + \frac{\tan^2(\phi)}{4Q_n^2}} \right).$$

It is evident that the center frequency differs from the natural frequency by a factor that is dependent on the nonresonant phase shift  $\phi$ . This effect is least for  $\phi = 0$  and grows rapidly beyond some angle depending on  $Q_n$ . For moderate values of  $Q_n$ , this breakpoint is beyond  $\phi \approx 60^\circ$ .

## VI. ANALYZING THE MODEL WITH THE PARAMETER $G$

We are now in a position to use the expression for  $G$  to probe the characteristics of the oscillator model. This will allow us to

verify the accuracy of the parameter against the known model performance. For the model oscillator, the expression for  $G$  is

$$G = \frac{i\omega(\omega_n/Q_n)Ae^{i\phi}}{\omega_n^2 - \omega^2 + i\omega(\omega_n/Q_n)}.$$

This expression is recognized as the canonical second-order bandpass response with a gain of  $Ae^{i\phi}$ . The frequency at which the angle of  $G$  crosses zero is given by

$$\omega_o = \omega_n \left( \frac{\tan(\phi)}{2Q_n} + \sqrt{1 + \frac{\tan^2(\phi)}{4Q_n^2}} \right)$$

which is precisely the oscillation frequency as determined for the model. The gain at this frequency is

$$G_0 = A \cos(\phi) = \Re(Ae^{i\phi}).$$

This result indicates that, in this example, only the real part of the amplifier gain contributes to the effective loop gain.

The loaded  $Q$  is computed by considering the phase slope at this frequency [12], which is related to the group delay by

$$Q = -\frac{1}{2}\omega_o \frac{\partial\varphi}{\partial\omega} = \frac{1}{2}\omega_o t_d.$$

Applying this to the expression for  $G$  gives

$$Q = \frac{\omega_o}{\omega_n} Q_n \cos^2 \phi - \frac{1}{4} \sin(2\phi) \approx \frac{\omega_o}{\omega_n} Q_n \cos^2 \phi.$$

It is seen that the computed  $Q$  is lower than the resonator  $Q_n$  by a factor that depends on the phase offset. For moderate values of  $Q_n$ , the factor is closely approximated by  $\cos^2(\phi)$ .

## VII. EXAMPLE

A practical oscillator is considered for analysis using the parameter  $G$  and the virtual-ground technique. This example will serve to illustrate the general analysis procedure. The numerical results obtained will later be compared with a SPICE simulation as a test of validity.

The general procedure is as follows. The oscillator schematic is recast by choosing a new virtual ground for the equivalent ac network. The loop is then broken in an appropriate place to form a two-port network for analysis. The parameter  $G$  is computed from the resulting *S*-parameter characterization. From  $G$ , oscillation frequency, stability, startup time, and loaded  $Q$  can be predicted.

The virtual-ground technique is to be applied to the Colpitts oscillator shown in Fig. 6. A full discussion of the virtual-ground technique is beyond the scope of this paper. Very generally, the virtual-ground point is typically chosen to arrive at a network that most resembles a cascaded amplifier and tuned circuit, and to minimize the reverse transmission coefficient,  $S_{12}$ . These two goals have been empirically found to best illuminate the fundamental mechanism underlying the operation of the oscillator being studied. Often this amounts to choosing the emitter or source of the active device as the virtual-ground point and lumping all of the passive components together as the resonant network. However, the results obtained by this technique are independent of the split point chosen. Therefore, a well-chosen

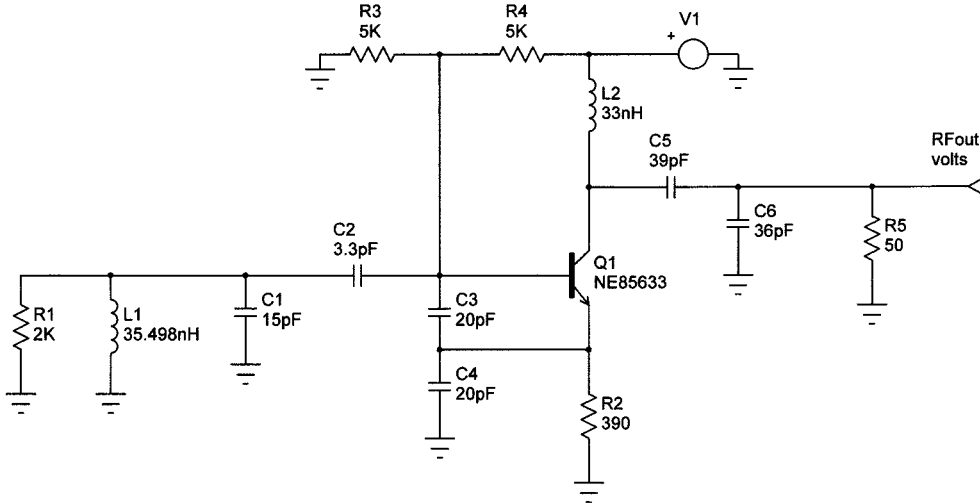


Fig. 6. Example oscillator. A Colpitts oscillator based on a bipolar device with collector-coupled output is used as an example. The schematic shown is ideal for SPICE simulation. However, before applying the virtual-ground technique, the circuit operation is arguably not intuitively obvious at first sight.

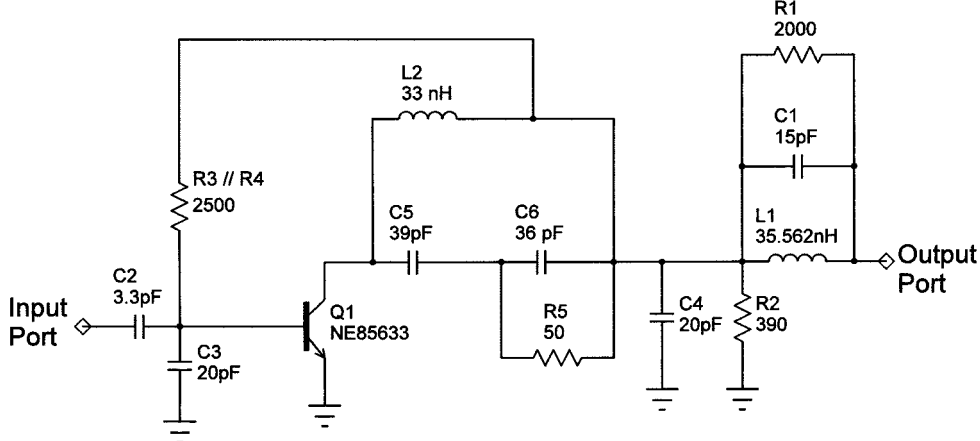


Fig. 7. Virtual-ground network for example oscillator. The example oscillator is redrawn in its equivalent ac form with the ground point defined at the emitter of Q1. In this example, the split point was chosen to point out the shortcomings of  $S_{21}$  rather than to enhance intuition as is typically done. However, this does not affect the outcome since  $G$  is independent of the split point.

split point is not required for accurate modeling. To illustrate this, the example oscillator was split at a less intuitive point. The resulting virtual-ground network is shown in Fig. 7.

The forward scattering parameter  $S_{21}$  of the virtual-ground network has typically been used to deduce oscillator performance with some success. The reason for this success is that, under certain conditions,  $S_{21}$  closely approximates  $G$ . It is interesting to examine the origins of this approximation to better understand its limitations. We start by expanding  $G$  to first order in  $S_{12}$  as follows:

$$G \approx \frac{S_{21}}{1 - S_{11}S_{22}} + S_{12} \left[ \frac{(S_{21} - 2)S_{21} - (1 - S_{11}S_{22})}{(1 - S_{11}S_{22})^2} \right].$$

Two effects seen from this approximation are primarily responsible for inaccuracies caused when using  $S_{21}$  alone. The zeroth-order term contains a factor that multiplies  $S_{21}$ . This factor approaches one when either or both  $S_{11}$  and  $S_{22}$  are small. However, if their product is not negligible,  $S_{21}$  may differ significantly from  $G$ . Second, the first-order coefficient is dominated

by a term proportional to  $S_{21}^2$ , which, by design, will not be negligible. Therefore, the first-order term is negligible only if  $S_{12}$  is small. Both of these conditions can sometimes be met with the proper choice of normalizing impedance and split point. If so,  $S_{21}$  alone can be used to determine oscillator performance.

A linear simulation is now performed to determine the  $S$ -parameters of the open-loop virtual-ground network of Fig. 7. From this, the magnitude and phase of  $G$  is computed as shown in Fig. 8.

There are two phase zero crossings in the Bode plot. The first phase zero crossing occurs with negative slope and positive gain. The second occurs with positive slope, but negative gain. This corresponds to one net clockwise encirclement of the point  $1 + j0$ . This indicates, according to the Nyquist criteria, that the closed-loop network will oscillate. From the intuitive arguments made earlier regarding startup time, we can deduce that the oscillations will be at the frequency of the negative slope phase crossing. The positive slope phase crossing will not support oscillations since the gain is less than one at that frequency.

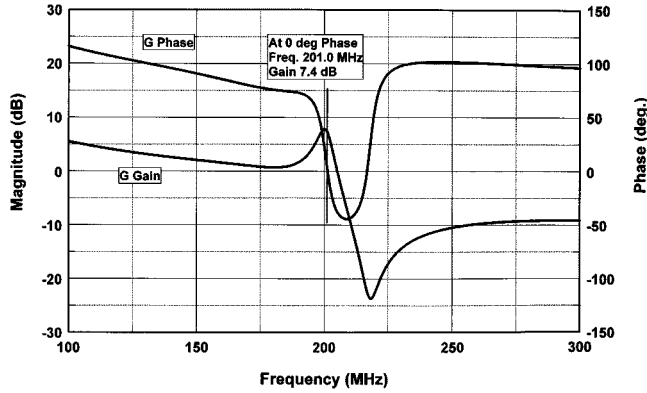


Fig. 8.  $G$ : linear simulation. The magnitude and phase of  $G$  is plotted as a function of frequency near the phase zero crossing for the virtual-ground network. Two phase zero crossings occur, but with different slopes (see text for interpretation).

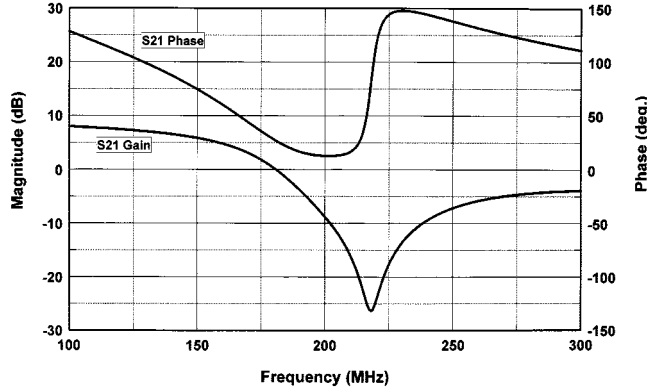


Fig. 9.  $S_{21}$ : linear simulation. The magnitude and phase of  $S_{21}$  is plotted as a function of frequency near the phase zero crossing for the virtual-ground network. Note that  $S_{21}$  does not exhibit a phase zero crossing; therefore, incorrectly indicating that the circuit would not oscillate.

From the figure, it can be seen that the frequency of the negative slope phase zero crossing is 201 MHz. The time delay at that zero crossing is 39.1 nS and the gain is 7.4 dB. This leads to an estimated 10–90 rise time of 100 ns. The loaded  $Q$  is estimated at 24.7.

In this case,  $S_{21}$  proves to be an extremely poor approximation to  $G$  as can be seen in Fig. 9. In fact, from  $S_{21}$ , one would deduce that the network would not oscillate.

### VIII. VERIFICATION

To verify the accuracy of the technique, a SPICE simulation was performed on the example oscillator circuit of Fig. 6. The  $S$ -parameters of the active device used in the linear simulation were generated using the SPICE model to ensure a consistent basis for comparison.

Startup time was determined from the SPICE simulation by direct measurement of the transient time-domain response of the circuit. The output of the transient simulation is shown in Fig. 10. From this graph, the 10–90 rise time was measured as 134 ns. Since nonlinearities cause the exponentially growing signal to eventually stabilize, the envelope was extrapolated, as shown in order to measure the 90% time. The frequency of oscillation was determined by counting cycles in the steady-state

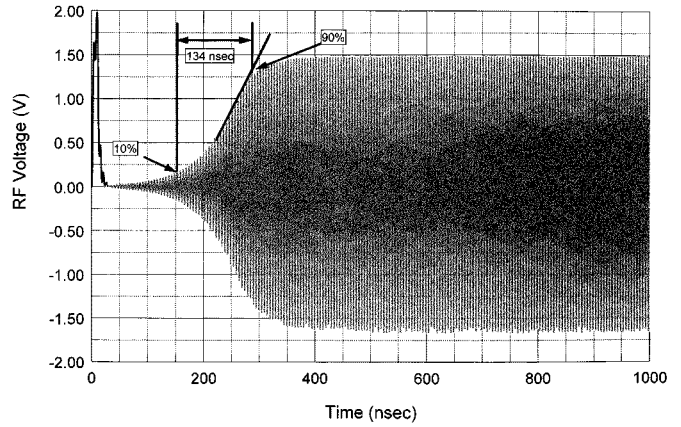


Fig. 10. Transient SPICE simulation. The output of the transient analysis for the example oscillator is shown. The exponential growth was extrapolated for comparison with the theoretical prediction.

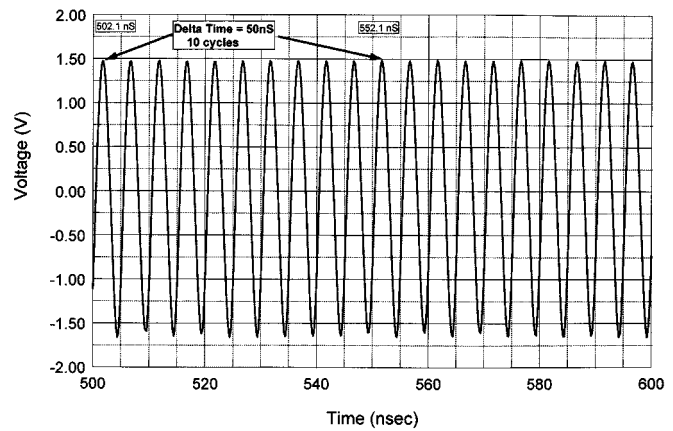


Fig. 11. Steady-state SPICE simulation. A steady-state region of the transient analysis for the example oscillator is shown. Frequency was determined by measuring the period of ten cycles.

TABLE I  
COMPARISON OF RESULTS OF ANALYSIS USING  $G$ ,  $S_{21}$  (NORMALIZED TO  $50 \Omega$ ), AND SPICE SIMULATION. IN THIS EXAMPLE,  $S_{21}$  PREDICTS NO OSCILLATIONS. THE PREDICTIONS OF THE SPICE SIMULATION MATCHES WELL WITH THAT OBTAINED FROM  $G$

	SPICE	$G$	$S_{21}$
Frequency	200 MHz	201 MHz	INVALID
Startup time	134ns	100ns	INVALID
Loaded Q	-	24.7	INVALID
Gain	-	7.4 dB	INVALID

graph of Fig. 11. The simulation indicated oscillations at a frequency of 200 MHz. Measurement of the loaded  $Q$  was not addressed with the SPICE simulation.

The time step used for the simulation was selected to ensure accuracy by the following method. The time resolution was increased in successive simulations. The results of each simulation were compared. It was found that the results converged to a final value beyond a particular resolution. The time step was

chosen to be just beyond this point and it is assumed that higher resolution is unnecessary.

## IX. CONCLUSION

A parameter  $G$  was derived that can be used to accurately predict the performance of an oscillator in conjunction with the virtual-ground technique.  $G$  can be expressed in terms of  $S$ -parameters resulting from a linear simulation of the two-port open-loop oscillator network. The parameter was shown to obey the same characteristic equation as derived through circuit analysis. Therefore, the Nyquist criteria can be applied to  $G$  to precisely determine oscillator stability. The oscillator performance characterized by  $G$  was analytically shown to match a simple oscillator model.

An example oscillator was analyzed using the virtual-ground technique with the parameter  $G$  and a SPICE simulation. The excellent agreement between the methods validates the theory. In addition, the example points out the limitations of using  $S_{21}$  in the virtual-ground technique.

The results of both analysis techniques are summarized in Table I.

## REFERENCES

- [1] S. Alechno, "Analysis method characterizes microwave oscillators," *Microwaves RF*, vol. 36, no. 11, pp. 82–86, Nov. 1997.
- [2] D. J. Esdale and M. J. Howes, "A reflection coefficient approach to the design of one-port negative impedance oscillators," *IEEE Trans. Microwave Theory Tech.*, vol. MTT-29, no. 8, pp. 770–776, Aug. 1981.
- [3] G. Strid, "S-parameters simplify accurate VCO design," *Microwaves*, vol. 14, no. 5, pp. 34–40, May 1975.
- [4] W. El-Kamali, J. Grimm, R. Meierer, and C. Tsironis, "New design approach for wide-band FET voltage-controlled oscillators," *IEEE Trans. Microwave Theory Tech.*, vol. MTT-34, pp. 1059–1063, Oct. 1986.
- [5] B. Parzen, "Universal, computer facilitated, steady state oscillator, closed loop analysis," in *IEEE Int. Freq. Contr. Symp.*, 1996, pp. 912–919.
- [6] D. E. Philips, "Computations of oscillator open-loop bode plots," in *45th Annu. Freq. Contr. Symp.*, 1991, pp. 336–340.
- [7] R. D. Martinez and R. C. Compton, "A general approach for the  $S$ -parameter design of oscillators with 1- and 2-port active devices," *IEEE Trans. Microwave Theory Tech.*, vol. 40, pp. 569–574, Mar. 1992.
- [8] R. W. Jackson, "Criteria for the onset of oscillation in microwave circuits," *IEEE Trans. Microwave Theory Tech.*, vol. 40, pp. 566–569, Mar. 1992.
- [9] N. M. Nguyen and R. G. Meyer, "Start-up and frequency stability in high-frequency oscillators," *IEEE J. Solid-State Circuits*, vol. 27, pp. 810–820, May 1992.
- [10] R. S. Carson, *High-Frequency Amplifiers*. New York: Wiley, 1982, p. 200.
- [11] J. J. D'Azzo and C. H. Houpis, *Linear Control System Analysis and Design*. New York: McGraw-Hill, 1981, pp. 283–300.
- [12] R. W. Rhea, *Oscillator Design & Computer Simulation*. Englewood Cliffs, NJ: Prentice-Hall, 1990, p. 47.

**Mitch Randall** received the B.S.E.E. degree from Iowa State University, Ames, in 1984, the M.S.E.E. degree and M.S. degree in physics from the University of Colorado, Boulder, in 1989 and 2000, respectively, and is currently working toward the Ph.D. degree in physics at the University of Colorado.

Since 1989, he has been with the National Center for Atmospheric Research, Boulder, CO, where his focus has primarily been on atmospheric remote-sensing instruments. He holds several patents spanning a range of topics, including antennas, signal processors, and high-power RF amplifiers.

**Terry Hock** (S'81–M'81) received the B.S. and M.S. degrees in electrical engineering from the University of Colorado, Boulder.

Since 1982, he has been a Research and Development Engineer at the National Center for Atmospheric Research (NCAR), Boulder, CO. He is also the Head of the Sounding Group, which develops balloon born instruments, and dropsondes for hurricane research. His research interests include frequency synthesizers, low-phase-noise voltage-controlled oscillators (VCOs), and wireless RF system design. He holds one patent for a balloon tracking antenna system.

Mr. Hock was the recipient of three NCAR Technical Achievement Awards.